Determining Area Affected by Dust Storms in Different Wind Speeds, Using Satellite Images (Case Study: Sistan Plain, Iran)

M.R. Ekhtesasi[a*], Z. Gohari[b]

[a] *Associate professor, Yazd University, Yazd, Iran*
[b] *MSc. Graduate, Yazd University, Yazd, Iran*

Abstract

The aim of this study is to determine the area affected by dust storms in different wind speeds using satellite images. In the first step, windy conditions of the Sistan plain were analyzed using wind statistics data. Next, five stormy days of Zabol city, indicating different wind speeds and horizontal visibilities during those storms, were selected. Then, high temporal resolution MODIS data was used as appropriate satellite data in this study. After that, a storm index was defined by means of analyses of storm radiance profile in bands with maximum and minimum storm reflection. The index is the square of difference between visible and thermal infrared bands, which is able to segment stormy confines with the range of reflection changes between 0 and 16. The reflection values were segmented in center of a 1 km^2 network using usual interpolation methods such as Local Polynomial, Radial Basis Function, Inverse Distance Weighted, Ordinary Kriging and Universal Kriging. In order to assess the above mentioned interpolation methods, validation techniques were applied using ArcGIS 9.2 software. The result of these assessments such as standard deviation method indicates that the Ordinary Kriging had lower standard deviation. By analyzing the variograms and spatial analysis of the data using GS$^+$ software, the best mathematic model able to fit the points was selected and classification was done by using this model. Finally, the stormy corridors with different dust densities were determined and by calculating the area and determining the villages located in these corridors, the critical regions were recognized. In this study the data from visible bands (4 and 9) and thermal band (21) of the MODIS sensor shows better results compared with the other bands, to segment and classify relative density of dust storms. Moreover, variographic analysis of the satellite data indicates that in most of the dust storms, power models with spherical threshold is the best for interpolation.

Keywords: Dust storm; Dust density; Remote sensing; Geostatistics; Kriging

1. Introduction

Dust storms in Sistan plain and Zabol city have had terrible consequences in recent years, especially during the recent droughts period in this region, in which regional Sadobistrozeh winds (120-day wind) of Sistan have been replaced by dust storms. Each event of dust storm brings forward a mass of dust to the cities that causes a lot of damages and jeopardizes people's health. The dust density of this phenomenon is not yet seriously analyzed and measured. So determining the ranges of dust

density during storm seems necessary for the future actions, and can be considered as an effective movement toward reducing costs of wind erosion control projects. Chomette et al, (1999) segmented area of the dust storm phenomena using IDDI (Infrared Difference Dust Index). This index is effective for the purpose of reducing thermal infrared radiance due to dust existence in the atmosphere. Calculated IDDI images are able to show clean atmosphere through comparing it with basic (no dust) image.

Xianjun et al, (2007) used thermal-infrared bands of MODIS images in order to analysis dust storm. In this study TIDI (Thermal Infrared Dust Index) was derived through quantitative analysis of MODIS data and was used to

---

* Corresponding author. Tel.: +98 913 3536617,
Fax: +98 351 8210312.
   E-mail address: mr_ekhtesasi@yazd .ac.ir

analyze storms event from 2004 to 2006 in Atlantic Ocean. This index is related to AOT (Aerosol Optical Thickness) with correlation coefficient higher than 76%. AOT is in 550 nm (Nanometer) domain and is closely related to emissivity and brightness of bands 20, 30, 31, 32 of MODIS images in such way that positive emissivity and brightness difference of bands 31 and 32 and high values of AOT index indicate high density of dust. Similarly, the average AOT and negative emissivity and brightness differences indicate less density of dust in storm.

Ochirkhuyag et al (2008) studied dust storm in Mongolia plain due to high frequent of the event in this area. The survey was done in 3 days from 6th to 9th of March 2006 using thermal infrared bands of NOAA and AVHRR and also reflective bands of Terra satellite. To have a better recognition of the storm, brightness temperature difference index (BTDI) was used. This index is the result of difference between CH_{32} and CH_31 bands of MODIS satellite and also difference between CH_5 and CH_4 bands of AVHRR satellite.

Some authors such as Bidokhti and Boroumand (2005), Mashhadi and Feiznia (2008) and Bidokhti et al (2002) investigated the effect of wind strength on wind threshold velocity and sand transition rate in different desert regions of Iran.

Mei et al (2008) investigated dynamic processes of dust storm using MODIS images. This survey was done in April 2006 based on absorption and reflection of dust storm as well as stimulating storm movement using various thermal data. The results were consistent with the survey done by meteorology organization. This Present study used BTDI to determine storm intensity.

Iranmanesh and Arabkhedry (2005) used MODIS images of Sistan plain's dust storms aiming to recognize detachment zone and the way they are distributed. To this end, images of this sensor in 2001 as well as landsat7 images were assessed to calculate vegetation index. The results indicated that the major detachment zone of dust particles is a dried Hamoon Sabory lake. The storm paths stretch to Iran, Afghanistan and Pakistan through separate and parallel corridors, one with high dust density and the other with low dust density.

2. Materials and Methods

2.1. The study area

Zabol plain is located in the northeast of Sistan and Baluchestan province. Its area is about 25000 km^2, 40% of which is in Iran and 60% in Afghanistan. The Hirmand river is the only water resource of Sistan plain which starts from Hendokosh and Baba Yaghma mountain in the northeast of Zabol, and joins Hamoon lake (Figure 1). Wind erosion has intensified due to present drought and dry of extensive bed of Hamoon's lakes and its grass lands. This area located on the path of 120-day-winds of Sistan region and drought crisis have led the high frequency of dusty days and irreparable damages.
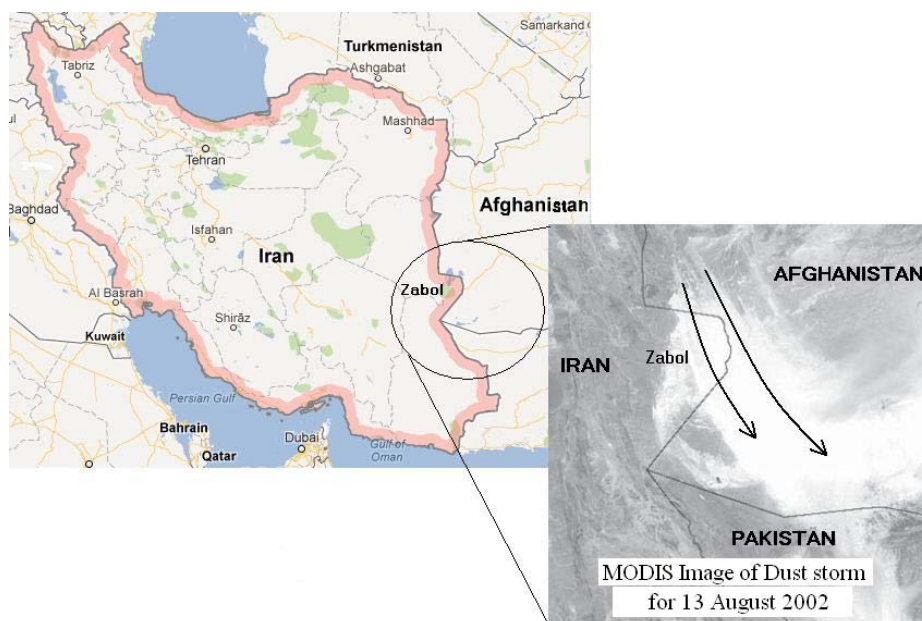

Fig. 1. The location map of study area in Sistan plain, Iran

2.2. Selection of satellite data

In the present study, stormy days were selected based on wind speed and horizontal visibility (HV) values of dusty days of Sistan plain. Then, based on the study objectives, five days representing storm with different speeds and horizontal visibility (Table 1) were selected.

August 13th, 2002 was selected to determine relative density of dust due to storm strength considering dust production and wind speed. The other dates of 2008 were determined aiming to storm classification. The codes (Julian day) referred to in the table 1 are related to the selected MODIS image dates.

Table1. Specification of the used images

Code	Date	Local	GMT	Max Wind Speed
225	2002/08/13	10:30	7	27
162	2008/06/10	10:30	7	18
172	2008/06/20	9:30	6	22
194	2008/07/12	10:30	7	24
223	2008/08/10	10	6:30	32

2.3. Geometric correction

Due to 1 km spatial resolution of MODIS images and storm on the selected image dates, level one MODIS data taken on August, 2002 was used for geometric correction. Geometric corrections of other images were done through image to image technique and controlled by means of topographical faces of the area in 1:250000 scale. After selecting control points and appropriate degree to change the coordinate system of image during geometric correction, It was calculated (RMS) for the coordinates of the selected points using Equation1:

$$RMS = ((x_1 - x_{org})^2 + (y_1 - y_{org})^2)^{0.5} \qquad (1)$$

where X_1 and Y_1 are the number of row and column of control points in the corrected image based on the pixel (Digital Number) to which the control point is correspondent. And X_{org},

Y_{org} are the numbers of the same control point in the corrected matrix.

2.4. Storm radiance profile

The radiance profile was used to present the best algorithm to segment and recognize storm in satellite images MODIS sensor possess 36 spectral bands in visible, infrared and thermal ranges. The marvelous capability of this sensor in spectral resolution makes it possible to segment and recognize faces by means of its images. Radiance profile in different bands (Figure 2) showed that in visible and infrared wavelength, radiance values are not significantly different but the band 9 has the maximum difference (least reflection in storm ranges). This study used this band and band 21 that has the maximum reflection in the storm range. After selecting appropriate bands, various methods were used to segment storm range which will be explained later.
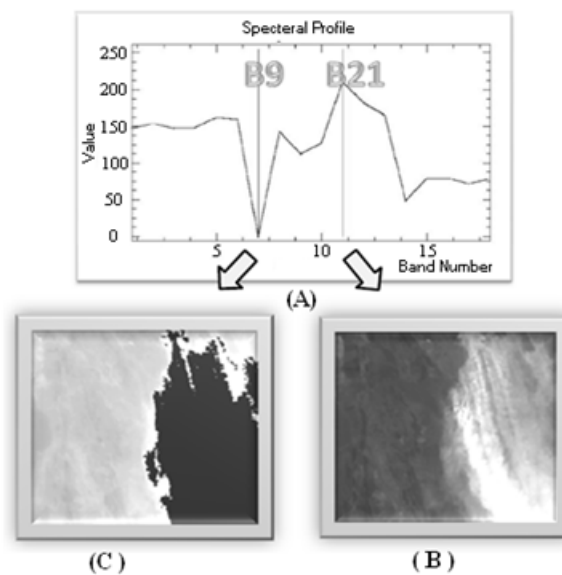

Fig. 2. A) Radiance profile for different bands of MODIS images, B) b21, Thermal infrared band, C) b9, Visible band

2.5. Storm index definition

In order to assess land surfaces, several models were created considering the properties of spectral reflection of land surface cover such as NDVI (Normalize Difference Vegetation Index). So, through algorithm and band ratio, it is possible to calculate index for phenomena such as storm which is able to segment storm according to different dust densities. The following equation was used to calculate infrared visible dust index:

$$IVDI = \sqrt{(b21 - b9)} \tag{2}$$

Where; b 21 is the recorded radiance in band 21 and b 9 is the recorded radiance in band9. This index varies from 0 to 16. IVDI (Infrared Visible Dust Index) was used to segment storm ranges. Figure 3 shows the ranges of the storms investigated in the present study which are segmented by IVDI.
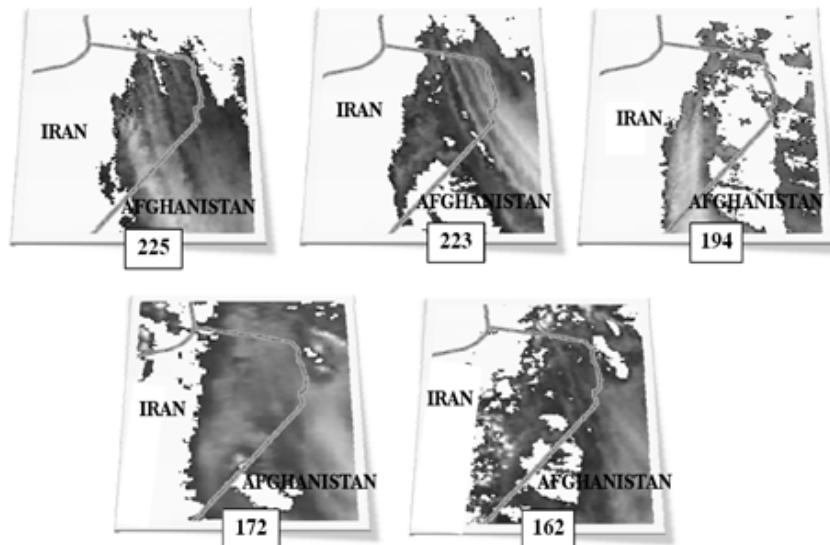

Fig. 3. Segmentation of stormy area by using IVDI

2.6. Extraction of digital number of images and investigation of data distribution normality

In the present study, calculated IVDI values for all pixels (with special resolution of 1 km) were used to analyse spatial correlation and determining optimal model to apply appropriate weight factor for interpolation. Digital numbers of images indicate dust density in the storms. In most of the interpolation methods it is necessary to establish normality hypothesis in data distribution. Normal distribution's graph is in bell form curve and completely symmetrical which is determined by statistical parameter of average, variance, skewness and kurtosis. In normal distribution skewness value varies from -1 to +1 and kurtosis from -3 to +3. In the present study, It was used normal QQ plot graph in ArcGIS software . After testing the normality of data by Kolmogorov- Smirnov method in Spss14 software, the normality of data was met and spatial analysis of them started. Table 2 shows the statistical parameters of storm investigated in the present study. Figure 4 shows normalization of the data.

Table 2. Determined statistical parameter of storms investigated

CODE	PIXEL	STDEV	AVERAGE	SKEW	KURT
162	21773	0.64	7.5	0.42	2.36
172	27177	0.94	8.41	0.17	2.41
194	15196	1.29	12.73	0.19	2.74
223	19253	0.77	9.43	0.48	2.4
225	19149	1.39	12.68	0.2	2

2.7. Interpolation methods

Estimation of quantity, in interpolation methods, It was done in 2 phases. In the first phase the variogram is delineated and the best model is fit on it. The spatial structure of the quantity would be analysed. The second phase is the estimation of quantity by means of interpolation methods which are based on model parameters of fitted variogram of the first phase.

In the present study, It was delineated the variograms for each of the storms after verification of data normality. Then Root Mean Square Error (RMSE) was calculated through the following methods: Local Polynomial (LP), Radial Basis Function (RBF), Inverse Distance Weighted (IDW), Ordinary Kriging (OK) and Universal Kriging (UK).

Precise estimators are those interpolation techniques able to estimate the values of a measured point with high level of accuracy. So, Kriging method was selected for classification considering minimum standard deviation using RMSE.
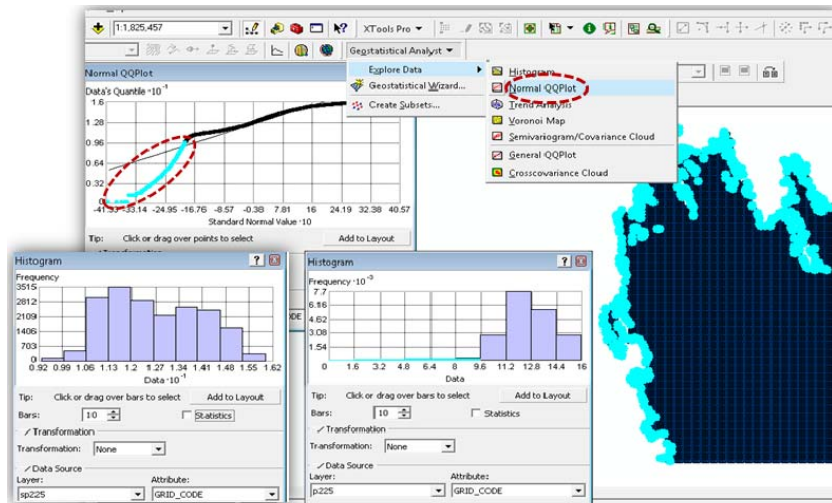

Fig. 4. The Method of data normalization

2.8. Variogram delineation

Geostatistics includes variography and interpolation processes. In variography process, variogram or distance dependant variance that shows the spatial relation structure among sample is used to model special variance of the data. Variogram function is defined as:

$$2\gamma^*(h) = \frac{1}{N(h)} \sum_{i=1}^{N(h)} [Z(x+h) - Z(x)]^2 \qquad (3)$$

Where $\gamma(h)$ is Semivariogram for N sample pair that are separated from each other with (h) distance. $Z(x)$ is the value of X variable in point i. Figure 5 shows the components of variogram.
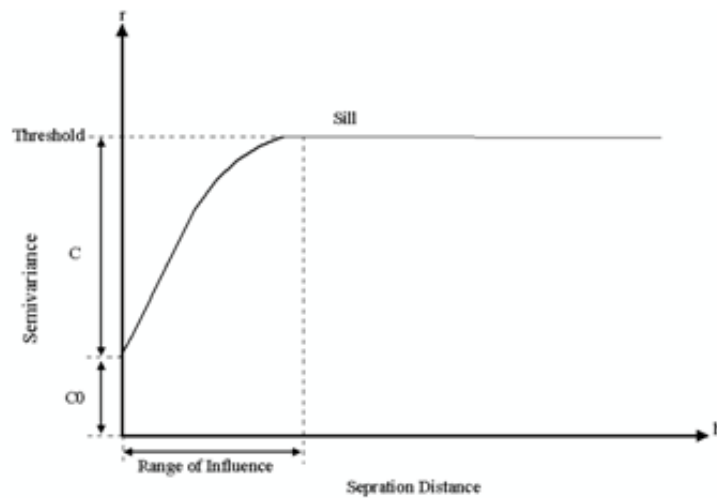

Fig. 5. Parameters of a typical variogram

Then the appropriate model with minimum square error was fitted to Semivariogram points and the parameters of Range, Sill and Nugget effect were calculated for interpolation analysis.

Models used for fitting on variogram points include Linear Model, Exponential Model and Spherical Models whose equations are:
Linear Model equation:

$$\gamma(h) = a.h + C0 \tag{4}$$

Exponential Model equation:

$$\gamma(h) = c\left[1 - e^{\frac{h}{a}}\right] + C0 \tag{5}$$

Sperical Model equation:

$$\begin{cases} \gamma(h) = c\left[\dfrac{h}{a} - 0.5\dfrac{h^3}{a^3}\right] + c0 & h < a \\ \gamma(h) = c + c0 & h > a \end{cases} \tag{6}$$

Where C is the threshold, C0 is Nugget effect and a is the Range.

To analyse and assess the models we applied cross validation method. This method includes omitting the sample in turn and reassessment them through Kriging using other samples and fitted model on experimental variogram. Then the different between real and assessed values were used to assess the estimations. Then the results from different estimators were compared through the following statistical criterions.

$$MSE = \frac{\sum_{i=1}^{n}[Z^*(x_i) - Z(x_i)]}{n} \tag{7}$$

$$RMSE = \sqrt{\frac{\sum_{i=1}^{n}[Z^*(x_i) - Z(x_i)]^2}{n}} \tag{8}$$

Where n is the number of observed points, $Z^*(x_i)$ is the estimated value in the point and $Z(x_i)$ is the observational value for the ith point. The best estimation in unobserved points is the estimation with the minimum MSE and RMSE. Kriging, which is a method to estimate or assess in geostatistics is the best estimator of unbiased linear able to estimate value of the variable in the area from which no sampling was done. With no base and minimum variance kriging function is defined as:

$$Z^* = \sum_{i=1}^{n} \lambda_i . Z(X_i) \tag{9}$$

Where Z^* the value of is estimated spatial variable, $Z^*(x_i)$ is the value of observed spatial variable in (x_i) and (λ_i) is the statistical weight given to x_i sample and indicate the importance of the ith point in the estimation. Normal distribution of Z variable is the condition that has to be met in order to use this estimator, otherwise we have to use either linear kriging or normalize the variable distribution.

3. Results

3.1. Interpolation method assessment

Table 3 shows the standard deviation in different interpolation methods.

Table 3. Comparison of Root of Mean Square Error in different interpolation method

Code	Root Mean Square Error (RMSE)				
	LP	RBF	UK	OK	IDW
225	0.19	0.16	0.18	0.16	0/18
223	0.09	0.08	0.11	0.08	0/10
194	0.34	0.33	0.36	0.32	0/35
172	0.11	0.11	0.1	0.09	0/11
162	0.1	0.11	0.09	0.09	0.12

3.2. Storm's variogram analysis

In the present study, spatial analysis and calculating experimental variogram were done through GS$^+$ software. The calculated variograms for the storms in this study have different shapes. In the variogram of storms 225 & 223 the intensity of the primary slop of variogram indicate the intensity of spatial changes of dust density which is a function of distance. Parabolic shapes near variogram origin indicate the high level of spatial coordinate in each variable. If the variogram be in the shape of a direct line (such as storm 225 variogram in Figure 6), with probability of crossing origin or possess nugget effect, such variograms do not have threshold and suggest the existence of

trend in the study area. Investigating reflections in images of storm 225 indicate that value of reflection that shows dust density increase with distance from storm origin.

The most ordinary variograms in geostatistics are those with threshold. If the variogram reach a certain sill and possesses a certain range, it has spatial structure and no trend.

The most ordinary variograms with sill is the spherical and exponential as shown in figure 6 on image date of 223, 194, 172 and 162. Both variograms have linear behaviour near origin, but the growth rate in spherical variogram is higher than exponential variogram. Exponential variograms never reach a certain threshold limit. The variogram of storm 223 is spherical.

Investigating image reflection also suggest that after passing a certain distance the values would be maximum, but the range of reflection changes in storms 162, 172 and 194 increase gently with distance. If variogram crosses the origin, it represents the complete continuous and if it does not cross the origin, it represents error. The lower the C0/C ratio, the greater would be the local correlation of data. Threshold value would be between 0 and 1. If C0/C is equal to 1, there won't be local correlation among variable. And if C_0/C is equal to 0 there will be a complete local correlation.

The parameters of different storm variograms are summarized in Table 4. Among the investigated storms, 194 & 225 possess minimum and maximum spatial correlation respectively.

Table 4. Variogram parameters of Case studied storms

Code	162	172	194	223	225
Model	Exponential	Exponential	Exponential	Spherical	Linear
Nugget (C0)	0.15	0.51	1.65	0.23	0.39
Sill (C+C0)	0.85	3.04	6.63	1.17	6.33
C/C_0	0.18	0.17	0.25	0.2	0.06
R^2	0.96	0.95	0.99	0.97	0.98
RMSE	0.96	2.23	7.9	3.1	1.5

Considering the delineated graph in figure 6 and statistical comparison in Table 4 for storms 194, 162 & 172 exponential model, storm 225 linear model and storm 223 spherical model with maximum correlation coefficient (>95%) and minimum error value, were selected as the best models.

These models are capable of reconstruction storm phenomena and producing map with more than 95% accuracy therefore they had high efficiency in determining stormy segments in the study area.
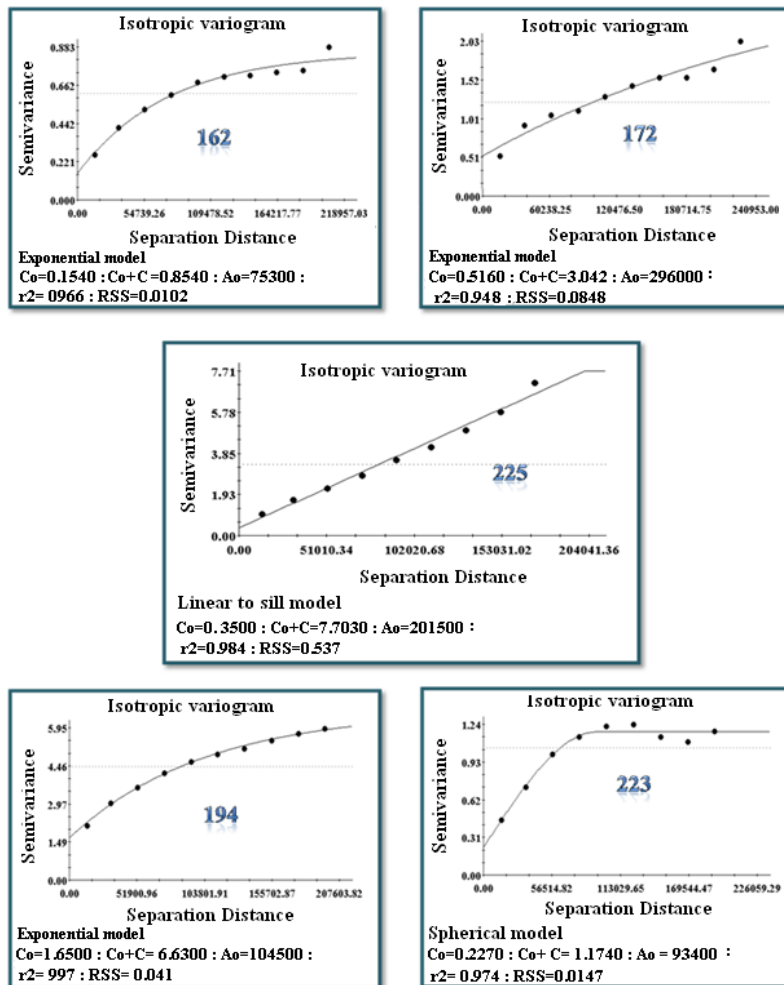

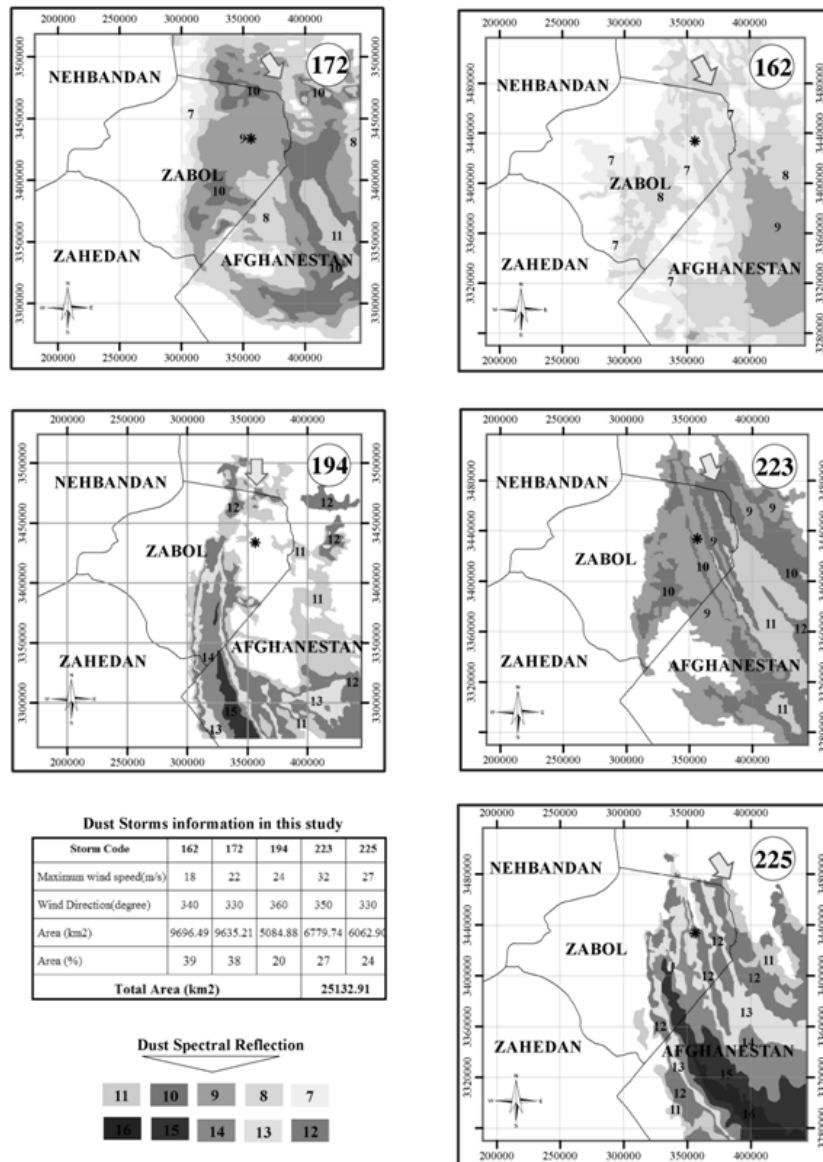Fig. 6. Evaluation of different variogram models in the surveyed

Dust Storms information in this study

Storm Code	162	172	194	223	225
Maximum wind speed(m/s)	18	22	24	32	27
Wind Direction(degree)	340	330	360	350	330
Area (km2)	9696.49	9635.21	5084.88	6779.74	6062.90
Area (%)	39	38	20	27	24
Total Area (km2)					25132.91

Dust Spectral Reflection

11	10	9	8	7
16	15	14	13	12

Fig .7. Dust density classification map in different wind speeds

4. Discussion and Conclusion

The obtained results, in different wind speeds, show that storm domain is different in the Sistan plain. On the other hand, dust density in each storm depends on wind speed and the type of storm. Generally, it can be classified frontal winds of Sistan plain into two major categories namely: ordinary front winds and hurricane-front winds. Ordinary front winds usually have higher speed but lower tensile strength while hurricane-front winds move upward and through the gap created in the front and crest of the storm drag with more dust upwards.

Although the wind speed is lower in this category, the density of the dust is higher. Investigation on the speed and direction of

winds in Zabol and Zahak stations indicates that, although wind speed in storm 223 is higher than other storms, dust density in storm 225 and 194 is higher. The major reason for that is the type of storm. Harat Mountains in Afghanistan and Birjand in Iran have created a natural wind corridor with NW to SW oriented, in such a way that this high pressure cyclones led to channelization and increase wind speed in this corridor. The results are consistent with the Iranmanesh & Arabkhedry(2005) and Rashki et al(2012) research. The shape of the dust storm is like U, generally. In severe storms, the role of natural corridor in canalization and increasing of density of dust storm is more evident.

In general, the dust sources, regardless of size or wind strength, are usually associated

with natural corridor in study region (Prospero et al., 2002).

The greatest dust activity takes place near a system of salt lakes and dry lakes found in the lowlands of the Hamoun basin, which is surrounded by arid-rocky mountains to its north and west. This region is associated with drainage features and extensive alluvial deposits, exhibiting some similarities with the lowlands south of the Atlas Mountains in northwest Sahara (Kahn et al., 2009) and Lake Eyre in Australia (Baddock et al., 2009).

Establishing reservoir dam on Hirmand River and exploiting water in Afghanistan have led to dehydration of ponds and preparing the ground for detachment of the sediments or in other words loading the storms. Low pressure Godezereh cyclone in Afghanistan makes the storms cyclic in this area. The results from dust storms classification indicate that the starting point of the storms is in Afghanistan and the maximum dust density during storm is in Godezereh pond in this country as well. It is worth mentioning that this issue has become a regional crisis for Iran, Afghanistan and Pakistan. As far as in extreme storms, the extent of the storms would continue to Pakistan.

The topographic condition of the region shows that the slop is sometimes near zero. Such low slop causes accumulation of water sediments resulted from erosion of upper basins and provide opportunity for extreme winds of the region to create the force necessary for sediments movement. Being surrounded by Babayaghma and Hendokush highlands and Darbandebad, Janja, Boz koh, Plang and, Doposht mountains in Iran has created special conditions in such a way that the western highlands near Sistan pediment through establishing natural wind corridors unidirectional with dominant winds as well as 120-day winds of East of Iran, causes channelization of wind in the valise among highlands.

Investigating on the villages and their location in stormy range of storm 225 suggests that, from the total 1101 villages in the study area 127 villages are out of the dusty corridor, 550 villages are in the medium dusty corridor, 423 villages are in high dusty corridor and 1 village (Shahr-e-Sukhte) is in super high dusty corridor. In this investigation Zabol and Zehak are also in medium dust corridor but the condition of 423 villages as well as Shahr-e-Sukhteh located in dense and super dense dust corridors respectively are critical. The condition of these villages in other storms with wind direction of 330 degree is the same.

In the present study the data from visible bands (4 and 9) and thermal band (21) of the MODIS sensor presented better results, comparing to other bands, to segment and classify relative density of dust storms. Selection of these bands was done after delineation of storm radiance profile that had maximum reflection of stormy range in bands 21 and 4, and minimum reflection of stormy range in band 9. As far as images of some storms did not have band 21 or the stripping noise of this band could not be removed through software techniques, we used band 4 in IVDI. It is worth mentioning that digital numbers of bands (4 and 21) were tested in IVDI and no significant different was found.

On one hand using satellite images in order to monitor natural phenomena such as storms is appropriate due to reducing the costs and saving time. On the other hand, in continues monitoring of surfaces covered by dust during storm, we need sensor with periodic xerography. Considering the importance of dust storms in different environmental, climatic and even economic discussions, we attempted to determine dust levels in storms with different wind speeds in Sistan pediment through MODIS images. Easy access to remote sensing data due to variety of the informative bands positioned this technique prior to air photos in the recognition of natural phenomena.

Appropriate distribution of the station or sampling locations and determining numerical data of IVDI to establish and develop prediction models are very important in the studies that need producing interpolation maps and determining spatial changes. The basis to delineate variograms in geostatistical methods is the points that are measured through field visit. Higher number of points and more appropriate locations can lead to more trustable fitted models. In the regions with no station or where the number or distribution of the stations are not appropriate (such as the study area) we have to use remote sensing data. So we suggest that in the similar studies, it is better to use combination of geostatistics and remote sensing data.

Geostatistics is a method that depends on models, so all of its layouts in kriging phase depend on variogram structure and its components. Nugget effect plays an important role in this regard. The variable investigated in the present study has low nugget effect. The reason can be the number of samples and their appropriate distances. Selection of best variogram pattern to use in kriging was done through estimation, verification and error

analysis. In order to analyse the fitted pattern we used MSE & RMSE. Variographic analysis on satellite data suggests that in most of the dust storms, power models with spherical threshold is the best for interpolation.

References

Alavipanah.K, K. Matinfar, A. Rafiei emam, 2008, Application of GIS in earth science, Tehran University.

Allexandra.k and Bullock.G, 1999, A comparative study of interpolation methods for mapping soil properties, Agronomy Jurnal, 91: 393-400

Baddock, M.C., Bullard, J.E., Bryant, R.G., 2009. Dust source identification using MODIS: A comparison of techniques applied to the Lake Eyre Basin, Australia. Remote Sens. Environ. 113, 1511–1528.

Bidokhti A. A., Boroumand N., 2005. Study of gap winds in the Lut Plateau. Desert Journal, 13(1).13-30.

Bidokhti A. A., Malekifard F. and Mirrokni M., 2002. a numerical model for prediction of threshold velocity of moving sand transport in deserts. Desert Journal,8(1). 127-136.

Chomette, O., Legrand, M and Marticorena, B, 1999, Determination of the wind speed threshold for emission of desert dust using sattellite remote sensing in the thermal infrared, Journal of Geophysical Research, 104: 31207- 31215

Fan Yi Da, Shi Pei Jun 1,Wang Xiushan 2, PAN Yao Zhong, (2002), The Analysis of Typical Dust Storm In Northern China By Remote Sensing, Advance In Earth Sciences

Fayyaz.M, 2005, The study on sand storms directions from detachment to deposing area on Sistan plain by use of satellite images. Proceedings of 1th national conference on wind erosion, Yazd- Iran.

Ginoux.P, Garbuzov.D,Hsu.C, 2010, Identification of anthropogenic and natural dust sources using Moderate Resolution Imaging Spectroradiometer (MODIS) Deep Blue Level 2 data. Journal of Geophysical Research, Vol. 115.

Gohari.Z, 2009, Mapping of relative dust density by use of satellite images (Case study: Sistan plain), Msc proposal, Yazd University.

Goroch, A., Burk, S and Davidson, K.L., 1980, Stability effects aerosol size and height distribution, Tellus, 32: 254-250

Goudie A. S., Middleton N. J. (eds), (2006) Desert Dust in the Global System, Springer, 288 p.

Hasanipak.A, 1997, (eds), Geoestatistic, first edition, Tehran university.

Huang, J., J. Ge and F. Weng (2007), Detection of Asia dust storms using multisensor satellite measurements. Remote Sensing of Environment 110 (2), 186-191

Iranmanesh.F, Arabkhedry. M. 2005, The study on detachment and origin of dust storms on Sistan plain by use of satellite images. Proceedings of 1th National conference on wind erosion, Yazd- Iran.

Kahn, R., Petzold, A., Wendisch, M., Bierwirth, E., Dinter, T., Esselborn, M., Fiebig, M.,Heese, B., Knippertz, P., Muller, D., Schladitz, A., Von Hoyningen-Huene, W., 2009. Desert dust aerosol air mass mapping in the Western Sahara, using particle properties derived from space-based multi-angle imaging. TellusB 61, 239–251.

Mashhadi N, Feiznia S., 2008. The study of removal (detachment) and transitional regions of wind erosion upon ground indicator (Case study:Khartouran Erg). Desert Journal,13. 75-87.

Mei.D, Xiushan.L , Lin. L, WANG Ping, 2008. Dust storm process dynamic monitoring with multi temporal MODIS data, The International Archives of the Photogrammetry, Remote Sensing and Spatial Information Sciences. Vol. XXXVII. Part B7. Beijing.

Nasiri.A, 1997, Methodes of spectrumorphic and spatial classifications on mapping of land use and land cover, Agriculture ministry, Information and Informatics section.

Ochirkhuyag. L., Tsolmon, R. , 2008, Monitoring the source of trans-National dust storms in North East Asia, The International Archives of the Photogrammetry, Remote Sensing and Spatial Information Sciences. Vol. XXXVII. Part B7. Beijing.

Prospero, J.M., Ginoux, P., Torres, O., Nicholson, S.E., Gill, T.E., 2002. Environmental characterization of global sources of atmospheric soil dust identified with the Nimbus 7 total ozone mapping spectrometer absorbing aerosol product. Rev. Geophys. 40, 2–31.

Rashki, A., Kaskaoutis, D. G., Rautenbach, C. J., Eriksson, P. G., Qiang, M., & Gupta, P. (2012). Dust storms and their horizontal dust loading in the Sistan region , Iran. Aeolian Research, 5, 51-62. Elsevier B.V. doi: 10.1016/j.aeolia.2011.12.001.

Xianjun Hao, John J. Qu, 2007, Saharan dust storm detection using moderate resolution imaging spectroradiometer thermal infrared bands, Journal of Applied Remote Sensing, Vol. 1, 013510